Environ. Sci. Technol. **1999**, *33,* 163−168

Kinetics of Trichloroethene Reduction by Zerovalent Iron and Tin: Pretreatment Effect, Apparent Activation Energy, and Intermediate Products

CHUNMING SU*,† AND ROBERT W. PULS‡

National Research Council and U.S. Environmental Protection Agency, National Risk Management Research Lab, 919 Kerr Research Drive, Ada, Oklahoma, 74820

The degradation of trichloroethene (TCE) at 2 mg L^{-1} in headspace free aqueous solution by zerovalent iron (Fe^0) and tin (Sn^0) was studied in batch tests at 10, 25, 40, and 55 °C and HCl-treated Fe^0 and Sn^0 at 25 and 55 °C. Surface area normalized pseudo-first-order rate constants (k_{SA}) ranged from 0.44×10^{-3} to 4.3×10^{-3} h^{-1} m^{-2} L for Fisher Fe^0, 0.029×10^{-3} to 0.27×10^{-3} h^{-1} m^{-2} L for Peerless and Master Builders Fe^0, and 0.011×10^{-3} to 1.31×10^{-3} h^{-1} m^{-2} L for Fisher and Aldrich Sn^0. The Aldrich Fe^0 was the least reactive with k_{SA} values ranging from 0.0016×10^{-3} to 0.011×10^{-3} h^{-1} m^{-2} L. The HCl-washing increased metal surface area and observed rate constant (k) values but generally decreased k_{SA} values. The calculated apparent activation energy (E_a) using the Arrhenius law for the four temperature levels ranged from 32.2 to 39.4 kJ mol^{-1} for the untreated Fe^0 metals and 40.5−76.8 kJ mol^{-1} for the untreated Sn^0 metals. Greater temperature effect was observed for Sn^0 than for Fe^0. Our results indicate that TCE reduction by Fe^0 and Sn^0 is likely controlled primarily by chemical reaction-limited kinetics rather than by mass transport of the TCE to the metal surface. Both reductive β-elimination reaction and hydrogenolysis reaction are likely involved in the reduction of TCE by both Fe^0 and Sn^0.

Introduction

Recent investigations on reduction of chlorinated solvents by zerovalent iron (Fe^0) have shown promising potential for applying the technology to the in situ remediation of contaminated groundwater (*1, 2*). Numerous feasibility studies, pilot tests, and field scale demonstration projects have been initiated using granular Fe^0 as the reactive medium in permeable reactive barriers (*2, 3*). Tin (Sn^0) has also been studied in the batch test and has been found to produce HCl and CO_2 when it reacts with CCl_4 in water (*4*). The most important factors influencing the reductive dechlorination reaction are the reactivity of individual chemical contaminants and the available concentration of Fe^0 surface area. Other factors such as Fe^0 surface condition, pH, initial contaminant concentration, and flow or mixing rate are minor contributors to the kinetic control (*5, 6*).

Temperature is important in affecting the rates as well as in providing unique insights into the reaction mechanisms. Chemical processes tend to exhibit larger temperature dependence than do physical processes. For example, diffusion-controlled reactions in solution have rather low activation energies (E_a < 21 kJ mol^{-1}), whereas surface-controlled dissolution reactions of most silicate minerals have E_a values usually in the range 42−84 kJ mol^{-1} (*7*), and E_a values for chemisorption on surfaces are often of the order of 84 kJ mol^{-1} (*8*). Sivavec and Horney (*9*) reported E_a values (15−18 kJ mol^{-1}) for the reduction of chlorinated ethenes by several commercial Fe^0 metals over a temperature range from 10 to 34 °C, indicative of a diffusion-limited reduction rate. No detailed information was given on the types of Fe^0 metals and name(s) of chlorinated ethenes for which the E_a values were measured. Scherer et al. (*10*) reported $E_a = 55.9 \pm 12.0$ kJ mol^{-1} for the reaction of CCl_4 with Fluka Fe^0, and $E_a = 40.5 \pm 4.1$ kJ mol^{-1} for hexachloroethane with Fluka Fe^0 over a temperature range of 4−45 °C. These values are indicative of chemical reaction rate control rather than diffusion control (*10*). More studies are needed to resolve these discrepancies. Furthermore, the effect of temperature on TCE reduction by Sn^0 has not been reported. More information on the temperature effect on metal-enhanced dechlorination is necessary for characterizing kinetic control on the performance of remediation technologies based on zerovalent metals.

Another approach to derive reaction mechanisms is through identification of the reaction products and intermediates. Recent studies have generated more information on the distribution of intermediate products of chlorinated solvents reduction by Fe^0. Orth and Gillham (*11*) found the principal degradation products of TCE reacted with Fisher Fe^0 to be ethene and ethane, with minor amounts of VC, all three DCE isomers, and other C1−C4 hydrocarbons. They suggested that a cumulative six electron transfer occurs to produce ethene when the TCE molecule resides at the Fe^0 surface. Matheson and Tratnyek (*12*) suggested direct electron transfer from the Fe^0 surface to the CCl_4 molecule in the reduction processes. A sequential hydrogenolysis of PCE → TCE → *cis*-DCE → VC → ethene was proposed by Schreier and Reinhard (*13*). Roberts et al. (*14*) and Campbell et al. (*15*) proposed an additional pathway where reduction of vicinal polychlorinated ethenes by Fe^0 occurs via reductive β-elimination. Reaction pathways including both hydrogenolysis and reductive β-elimination were able to account for most of the observed products (*15*). These studies were generally performed at a single (room) temperature level such that there is little information available on the effects of temperature on both degradation rate and product distribution of chlorinated solvents reduction.

The objectives of this study were to (1) compare the reactivity of different types of Fe^0 and Sn^0 toward TCE; (2) study the effect of acid pretreatment of Fe^0 and Sn^0 on TCE degradation kinetics; (3) investigate temperature effect on TCE reduction rate; and (4) examine the distribution of major reaction byproducts.

Experimental Section

Chemicals and Materials. We used TCE (99+%, Aldrich, Milwaukee, WI), Fisher electrolytic Fe^0 (99%, 100 mesh, Fisher Scientific, Fair Lawn, NJ, Cat. No. I60-3), Aldrich Fe^0 (325 mesh, 97%, hydrogen reduced, Cat. No. 20930-9), Peerless Fe^0 (Peerless Metal Powders & Abrasive, Detroit, MI), Master Builders Fe^0 (Master Builders Inc., Cleveland, OH), Fisher powdered Sn^0 (Cat. No. T129-500), Aldrich powdered Sn^0 (325 mesh, 99.8%, Cat. No. 26563-2), Aldrich granular Sn^0 (30 mesh, ACS reagent), and HCl-washed Fe^0 and HCl-washed Aldrich powdered Sn^0. Preliminary tests showed that HCl-

* Corresponding author phone (580)436−8638; fax (580)436−8703; e-mail: su.chunming@epa.gov.
† National Research Council.
‡ U.S. EPA.

10.1021/es980481a CCC: $18.00
Published on Web 11/20/1998

TABLE 1. Surface Area Normalized Rate Constants (k_{SA}) and Activation Energies (E_a) (Mean ± Sample Standard Deviation) for TCE Reduction by Untreated (Calculated from All Four Temperature Data) and HCl-Washed (Calculated from 25 °C and 55 °C Data) Fe^0 and Sn^0

material	surface area, $m^2\ g^{-1}$	surface area normalized rate constants (k_{SA}) × 1000, $h^{-1}\ m^{-2}\ L$				activation energy, kJ mol^{-1}
		10 °C	25 °C	40 °C	55 °C	
Fisher Fe^0	0.091 ± 0.005	0.444 ± 0.034	1.102 ± 0.064	2.494 ± 0.231	4.313 ± 0.427	39.4 ± 3.6
Master Builders Fe^0	1.164 ± 0.047	0.0289 ± 0.0008	0.109 ± 0.004	0.156 ± 0.003	0.198 ± 0.006	32.2 ± 0.1
Peerless Fe^0	0.699 ± 0.055	0.0304 ± 0.0001	0.103 ± 0.000	0.198 ± 0.005	0.270 ± 0.019	37.4 ± 0.3
Aldrich Fe^0	0.192 ± 0.001	0.0016 ± 0.0000	0.0032 ± 0.0006	0.0063 ± 0.0032	0.011 ± 0.001	32.3 ± 1.9
Fisher powdered Sn^0	0.139 ± 0.003	0.0164 ± 0.0039	0.122 ± 0.002	0.162 ± 0.015	1.306 ± 0.045	69.3 ± 3.9
Aldrich powdered Sn^0	0.184 ± 0.006	0.0107 ± 0.0002	0.0481 ± 0.0025	0.181 ± 0.004	1.008 ± 0.042	76.8 ± 1.1
Aldrich granular Sn^0	0.068 ± 0.014	0.0177 ± 0.0011	0.0424 ± 0.0017	0.0733 ± 0.0046	0.207 ± 0.023	40.5 ± 0.2
$Fe^0 + Sn^0$ [a]	0.115 ± 0.004	0.0573 ± 0.0051	0.308 ± 0.018	1.017 ± 0.030	2.122 ± 0.084	62.5 ± 2.1
Fisher Fe^0 (HCl)	0.334 ± 0.028		0.308 ± 0.028		0.971 ± 0.176	31.0 ± 2.5
Master Builders Fe^0 (HCl)	2.136 ± 0.088		0.0690 ± 0.0116		0.178 ± 0.005	25.8 ± 4.0
Peerless Fe^0 (HCl)	1.269 ± 0.066		0.0344 ± 0.0011		0.108 ± 0.009	31.0 ± 1.3
Aldrich Fe^0 (HCl)	1.930 ± 0.069		0.0011 ± 0.0000		0.023 ± 0.002	81.8 ± 2.6
Aldrich granular Sn^0 (HCl)	0.031 ± 0.005		0.122 ± 0.008		0.355 ± 0.014	29.1 ± 0.5

[a] 7.5 g Fisher Fe^0 + 7.5 g Fisher powdered Sn^0.

washing of powdered Sn^0 resulted in massive cemented blocks of Sn^0 particles so we stopped acid pretreatment of powdered Sn^0. Pretreatment of metal filings was performed by washing 750 g of metals in 400 mL of Ar-sparged 1 M HCl with periodic shaking for 30 min and then rinsing 10 times with vigorous shaking in Ar-sparged deionized water to remove residual acidity and chloride. The washed metals were dried at 110 °C in an oven under Ar atmosphere. The dried metals were stored in Ar-sparged jars to inhibit oxidation. Metal surface area (Table 1) was determined by BET N_2 adsorption analysis on a Coulter SA3100 surface area analyzer (Coulter Co., Hialeach, FL). Both untreated and HCl-washed metals were examined under a scanning electron microscope (SEM).

Batch Tests. Fifteen grams of each metal were added to each 50-mL (with measured internal volumes of 60 ± 1 mL) clear borosilicate serum bottles (Weaton, Millville, NJ) that were then filled with TCE solution prepared with deionized water at about 2 mg TCE L^{-1} with no headspace. The bottles were sealed immediately with aluminum crimp caps with Teflon-lined septa. Two bottles containing TCE and metals and two controls containing TCE only were prepared for each sampling time period at 2, 4, 8, 12, 24, 48, 72, 96, and 120 h. Untreated metals were tested at four temperatures (10, 25, 40, 55 °C) and HCl-washed metals at two temperatures (25 and 55 °C) on a shaker set at 50 rpm in a water-bath. At preset sampling time intervals, 15 mL of subsamples were transferred via a glass syringe from the serum bottles to 40-mL (with measured internal volumes of 43.0 ± 0.6 mL) glass vials that were then filled with deionized water with no headspace and capped immediately using a Teflon faced septum and aluminum crimp cap for volatile organic compound analyses. Another subsample of 15 mL was removed via a glass syringe to a 20-mL (with measured internal volumes of 21.5 ± 0.2 mL) glass vial capped using a Teflon faced septum and aluminum crimp cap for dissolved gas analyses. Due to the sampling procedure employed, the gas analyses were only qualitative. The remaining solution was analyzed for Eh and pH and then filtered through 0.1 μm membrane for Fe^{3+}, Fe^{2+}, and Cl^- determination.

Analytical Methods. The concentrations of TCE and its chlorinated products were determined by automated purge and trap gas chromatography (GC). Samples contained in 40-mL glass vials were loaded into a Tekmar ALS 2050 autosampler (Tekmar, Cincinnati, OH). A 5 mL aliquot of sample was transferred via a sample loop into the purge vessel. The liquid sample was purged with He gas for 4 min to transfer volatile analytes onto a Carbopak/Carbosieve (Tekmar #8) trap. The trap was dry purged with He gas for 10 min to remove water vapor, and analytes were thermally desorbed for 4 min at 240 °C onto the GC column for separation and analyses. Sample transfer was through a heated 0.32 mm uncoated fused silica transfer line that was coupled directly to the analytical column. The transfer line/column connection was made with a low dead volume butt connector inside the GC oven. To separate analytes, a cryogenic cooling step was employed with an initial temperature of −80 °C, followed by an initial ramp of 10 °C min^{-1} to −30 °C, and then followed by ramp A at 2 °C min^{-1} to −10 °C with a final time of 4 min and ramp B at 15 °C min^{-1} to 230 °C with a final time of 5 min. The sequence of separation was as follows: VC, 1,1-DCE, *trans*-DCE, *cis*-DCE, and TCE. Following separation on the column, analytes were determined with a flame ionization detector on a Hewlett-Packard 5890 GC. The total run time for each sample was 40 min. The detection limit was 1.0 μg L^{-1} for TCE, 1,1-DCE, *trans*-DCE, and *cis*-DCE and 0.5 μg L^{-1} for vinyl chloride.

Dissolved ethene and ethane were estimated using a gas chromatography headspace equilibration technique. The sample was introduced into the MTI P200 GC equipped with a 10 m MS-5A capillary column and a 8 m Poraplot U capillary column via a built-in vacuum pump into the sample loops/injectors. A sample was injected into the two different capillary columns and detected by two independent thermal conductivity detectors. The detector signals were processed by a computer system interfaced with the GC. The quantitation limit for ethane, ethene, and acetylene was 10 mg dm^{-3} in the gas phase. By using Henry's law, the concentration of the gas in the solution was calculated. Ferric and ferrous ions were determined by high performance liquid chromatography (*16*) with detection limits of 0.03 and 0.09 μM, respectively. Chloride was determined by Waters capillary electrophoresis method N-601 and corrected for the background chloride in the metals. Redox potential and pH were determined with an Orion ion analyzer (Orion Research Inc., Boston, MA) by using a combination redox electrode and a combination pH electrode. The Eh readings were reported relative to the normal hydrogen electrode.

Results and Discussion

Surface Area Effect. Previous studies (*1, 5*) have shown that the rate of degradation of chlorinated solvents by Fe^0 follows a pseudo-first-order reaction with respect to contaminant concentration as depicted in eq 1 and with respect to the quantity of Fe^0 surface area as described in eq 2

$$\ln C = \ln C_o - k\,t \tag{1}$$

and

$$\ln C = \ln C_o - k_{SA}\rho_a t \quad (2)$$

where C is the TCE concentration (mg L^{-1}), C_o the initial TCE concentration (mg L^{-1}), k the observed rate constant (h^{-1}) and k_{SA} the surface area normalized reaction rate constant (h^{-1} m^{-2} L), ρ_a the surface area concentration of Fe^0 (m^2 L^{-1} of solution), and t the time (h).

The relationship between k_{SA} (or k) and temperature is described by a logarithmic expression of the Arrhenius equation

$$\ln k_{SA} = \ln A - E_a/RT \quad (3)$$

where E_a is the activation energy (kJ mol^{-1}), R the molar gas constant (0.008 314 kJ mol^{-1} K^{-1}), T the absolute temperature (K), and A is a preexponential factor (h^{-1} m^{-2} L). The activation energy for the reaction was obtained from the slope of a plot of ln k_{SA} vs $1/T$ using linear least-squares analysis (Table 1).

The amount of available surface area under an effectively constant metal surface condition is one of the most significant experimental variables affecting contaminant reduction rate (*17*). Figure 1 presents a linear relationship between the pseudo-first-order rate constant k ($k = k_{SA}\rho_a$) and the surface area of Peerless Fe^0 per unit solution volume (m^2 L^{-1}). Matheson and Tratnyek (*12*) obtained a linear regression line of k (min^{-1}) versus surface area concentration ρ_a (m^2 L^{-1}) for tetrachloride dechlorination by Fisher Fe^0: k (min^{-1}) $= 0.0025\rho_a + 0.017$. In both cases, the regression line does not go through the origin, implying that other loss processes such as adsorption (*18*) are contributing to the substrate disappearance.

Of the iron samples tested, Aldrich Fe^0 was the least reactive. A 3 orders of magnitude range in k_{SA} for different types of Fe^0 suggests that other factors such as iron impurity, crystallinity, and morphology may also be important factors affecting TCE reduction. Further study is needed to fully understand the involvement of these or other unknown factors.

HCl Pretreatment Effect. HCl-washing of metals generally resulted in an increase in specific surface area, which in turn led to a greater observed rate constant k for TCE reduction; however, the surface area normalized rate constants (k_{SA}) were decreased when the metals were HCl-washed with the exception of Aldrich Fe^0 at 25 °C and Peerless Fe^0 at 55 °C (Table 1). Aldrich granular Sn^0 had a decreased surface area after HCl-washing, which was caused by the loss of fine particles during the washing and rinsing process. Our results are consistent with previous studies (*11, 17*) that have shown accelerated dechlorination rates with dilute HCl treatment of the iron metal, despite the fact that the drying step used in the present study was not used by previous researchers (*11, 17*). Agrawal and Tratnyek (*17*) pointed out that the effect of HCl pretreatment may be due to one or more of the following changes: cleaning of the surface by dissolution of metal and breakdown of the passivating oxide layer; increasing the metal surface area by etching and pitting through corrosion; increase in the density of highly reactive sites consisting of steps, edges, and kinks, following corrosion by acid; and increased concentrations of adsorbed H^+ and Cl^- that persist after pretreatment with HCl. Additionally, the HCl-washing and drying processes may have generated more nonreactive sites relative to the reactive sites so that the k_{SA} decreased as a result of acid pretreatment.

Under scanning electron microscopy, the HCl-washed Aldrich Fe^0 displayed a rougher surface which was due to aggregates of small spheroidal particles on the surface. Some type of coatings scattered across the surface of Peerless and Master Builders Fe^0 appeared to have been largely removed by the acid wash. Untreated Peerless Fe^0 had a small amount of Si, Mn, C, and O on the surface as revealed by energy-dispersive X-ray spectroscopy. The HCl-washing appeared to have removed most of the graphite from the surface.

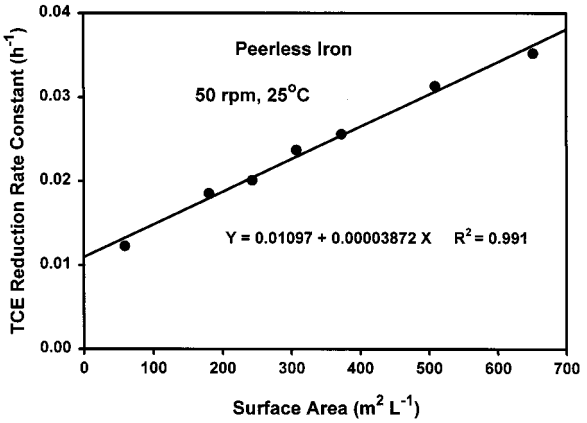

FIGURE 1. Observed pseudo-first-order rate constant (*k*) for TCE reduction by pristine Peerless Fe^0 as a function of Fe^0 surface area concentration. Tests were performed by varying mass of Fe^0 in serum bottles (60 mL by volume) in contact with 2 mg TCE L^{-1} solution at 50 rpm and 25 °C for time periods of 2, 4, 8, 12, 24, 48, 72, 96, and 120 h.

Temperature Effect. The E_a is a measure of the energy required to realize a process that is temperature dependent. In this case, E_a can be viewed as the quantity of energy the TCE molecule and Fe^0 (or Sn^0) must have in order to complete the reduction of TCE and oxidation of Fe^0 (or Sn^0). A few reaction steps may be involved in the overall reaction of TCE with the metals. First, TCE is diffused through the solution to a metal particle which is usually coated by a (hydr)oxide layer; second, TCE is adsorbed to a favorable reaction site on the metal particle; third, electrons are transferred from the metal to the TCE molecule forming intermediate products such as DCE isomers, chloroacetylene, VC, etc. and metal (hydro)oxides; fourth, the intermediate products are subsequently transformed to less chlorinated compounds; and fifth, some intermediate and final products diffuse from the metal surface to the solution. The slowest reaction step, that requires the greatest E_a, determines the kinetics of a reaction.

Scherer et al. (*10*) concluded that the rate of CCl_4 reduction by oxide-free Fe^0 appears to be dominated by reaction at the metal−water interface rather than by transport to the metal surface because their measured first-order heterogeneous rate constant for the chemical reaction was less than the estimated rate constant for mass transfer to the surface. However, they studied CCl_4 reduction at an Fe^0 rotating disk electrode in pH 8.4 borate buffer made from 0.15 M H_3BO_3 and 0.0375 M $Na_2B_4O_7$. Borate at 0.05 mM has been shown to strongly inhibit reduction of CCl_4 by Fe^0 (*19*); therefore, the measured rate constant for the CCl_4 reduction by Scherer et al. (*10*) could have been greater in the absence of the borate buffer. Nevertheless, our study seems to support their findings that surface-chemical reaction rather than diffusion is the limiting step in the dechlorination process as further discussed below.

Diffusion requires less energy than chemical reaction although there is no consensus in the literature on the typical E_a values for a diffusion process. Laidler (*8*) listed a value of 21 kJ mol^{-1}, Spiro (*20*) gave values in the range of 10−16 kJ mol^{-1} for mass transport-controlled reactions, while Pilling and Seakins (*21*) gave an $E_a \approx 15$ kJ mol^{-1} for diffusion-controlled reactions in water. In contrast, Sparks (*22*) stated that low E_a values (<42 kJ mol^{-1}) usually indicate diffusion-controlled processes, whereas higher E_a values indicate chemical reaction processes. In our discussion, an E_a value of 15 kJ mol^{-1} for diffusion-controlled reactions in water is chosen because it is the most often cited value. The activation

TABLE 2. Normalized Half-Lives ($t_{1/2-N}$, for 1 m^2 mL^{-1}) for TCE Degradation by Untreated and HCl-Washed Fe^0 and Sn^0

material	$t_{1/2-N}$, h			
	10 °C	25 °C	40 °C	55 °C
Fisher Fe^0	1.56 ± 0.13	0.64 ± 0.04	0.28 ± 0.03	0.16 ± 0.01
Master Builders Fe^0	24.1 ± 0.6	6.39 ± 0.23	4.44 ± 0.09	3.50 ± 0.10
Peerless Fe^0	40.8 ± 0.8	6.74 ± 0.01	3.51 ± 0.08	2.57 ± 0.18
Aldrich Fe^0	419 ± 7	214 ± 44	129 ± 66	63.1 ± 7.6
Fisher powdered Sn^0	43.7 ± 5.3	5.67 ± 0.07	4.29 ± 0.40	0.53 ± 0.01
Aldrich powdered Sn^0	64.4 ± 0.9	14.5 ± 0.8	3.83 ± 0.01	0.69 ± 0.03
Aldrich granular Sn^0	38.7 ± 2.8	16.4 ± 0.5	9.48 ± 0.62	3.36 ± 0.37
Fisher Fe^0 + Sn^0 (1:1)	12.2 ± 1.0	2.25 ± 0.13	0.69 ± 0.02	0.33 ± 0.01
Fisher Fe^0 (HCl)		2.26 ± 0.21		0.73 ± 0.13
Master Builders Fe^0 (HCl)		9.35 ± 1.58		3.59 ± 0.09
Peerless Fe^0 (HCl)		10.1 ± 0.3		3.23 ± 0.25
Aldrich Fe^0 (HCl)		211 ± 10		30.1 ± 2.9
Aldrich granular Sn^0 (HCl)		5.71 ± 0.33		1.96 ± 0.08

energies ranged from 32.2 to 39.4 kJ mol^{-1} for the four virgin Fe^0 and from 40.5 to 76.8 for the three virgin Sn^0, indicating that chemical reaction rather than diffusion is the predominant process (Table 1). Temperature effect was more significant for Sn^0 relative to Fe^0 as indicated by the larger E_a for Sn^0. The largest E_a for the HCl-washed Aldrich Fe^0 may be related to the 10-fold increase in surface area by HCl-washing. Acid washing resulted in slightly smaller E_a values for Fe^0 and Aldrich Granular Sn^0 with the exception of Aldrich Fe^0. Aldrich Fe^0 is made by hydrogen reduction and is less pure (97%) than Fisher iron (99^+%). The variation of E_a values among different untreated and HCl-treated metals could be a result of different reactive sites on the metal surface, impurities, structure, and morphology of the surface, etc. Thus, a range of E_a values does not mean that the same process (e. g., chemical reaction) could not be controlling the degradation of TCE in these systems.

Applications. The calculated normalized half-lives ($T_{1/2-N}$) of TCE differed by more than 2 orders of magnitude between Fisher and Aldrich Fe^0, whereas comparable results were obtained between Master Builders and Peerless Fe^0 (Table 2). A headspace developed in the Fisher Fe^0 serum bottles after 48 h at 25 °C, whereas no headspace was observed in the other untreated Fe^0 bottles even after 120 h at 25 °C. A headspace may have facilitated stripping loss of volatile constituents resulting in low carbon mass balance. The $T_{1/2-N}$ values decreased with increasing temperature with the greatest temperature effect shown between 10 and 25 °C. The TCE $T_{1/2-N}$ value for Peerless Fe^0 at 25 °C was 0.64 h, which compares well with a value of 0.67 h for a Fisher Fe^0 with a surface area of 0.287 m^2 g^{-1} from a similar batch test (*1*) (Table 2). A mixture of 50/50 by mass of Fisher Fe^0 and Sn^0 resulted in $T_{1/2-N}$ values between those for the 100% Fe^0 and Sn^0, indicating zero benefit by mixing the two metals. As temperature increased to 55 °C, the difference in $T_{1/2-N}$ values diminished between the Fe^0 and Sn^0 with the exception of Aldrich Fe^0.

Selection of an appropriate barrier width is one of the most critical considerations in the design of permeable reactive barriers. The barrier width must provide sufficient contact time to ensure that contaminants are degraded to target levels (*6*). The data of temperature-dependent K_{SA} have practical implications for in situ remediation of chlorinated solvents by permeable reactive barriers made with Fe^0. For the same reactive material, a thinner iron wall could be constructed in a warmer area than in a cold area. Furthermore, since the temperature of most groundwater ranges from a few to <20 °C and iron itself is a good heat conductor, it may be technically and economically feasible to increase the temperature near the iron wall to >25 °C by electrical or radio frequency heating. By doing so, contaminant degradation rates can be significantly enhanced, whereas the thickness requirement of the iron wall can be reduced.

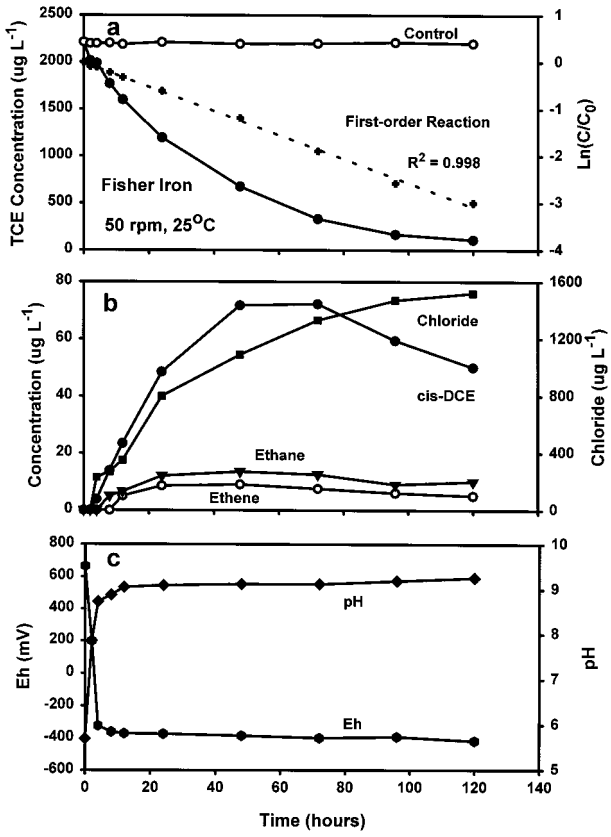

FIGURE 2. Kinetics of TCE reduction by pristine Fisher Fe^0 at 50 rpm and 25 °C: (a) TCE concentration and the pseudo-first-order equation fit of the data using a rate constant *k*, (b) reaction byproducts, and (c) pH and Eh.

Intermediate Products and Reaction Pathways. Figure 2 shows the batch test results for TCE reduction by Fisher Fe^0 at 25 °C. The TCE concentration in the control serum bottles was essentially constant over the entire time period, whereas an exponential decline of TCE concentration was evident with Fisher Fe^0, and the data was fit satisfactorily with a pseudo-first-order reaction equation. Reaction products included *cis*-DCE that exhibited a maximum between 48 and 72 h, ethene, ethane, and chloride (Figure 2b). A previous study has shown, as TCE degrades by Fe^0, the predominant chlorinated products are *cis*-DCE and VC, and 1,1-DCE is found at concentrations an order of magnitude below *cis*-DCE (*23*). The VC was generally not detected in the Fe^0 systems in this study. Another study has demonstrated that chloroacetylene is produced by β-elimination, and it is degraded quickly to acetylene or VC (*14*). No attempt was made to detect chloroacetylene in this study. Chloride

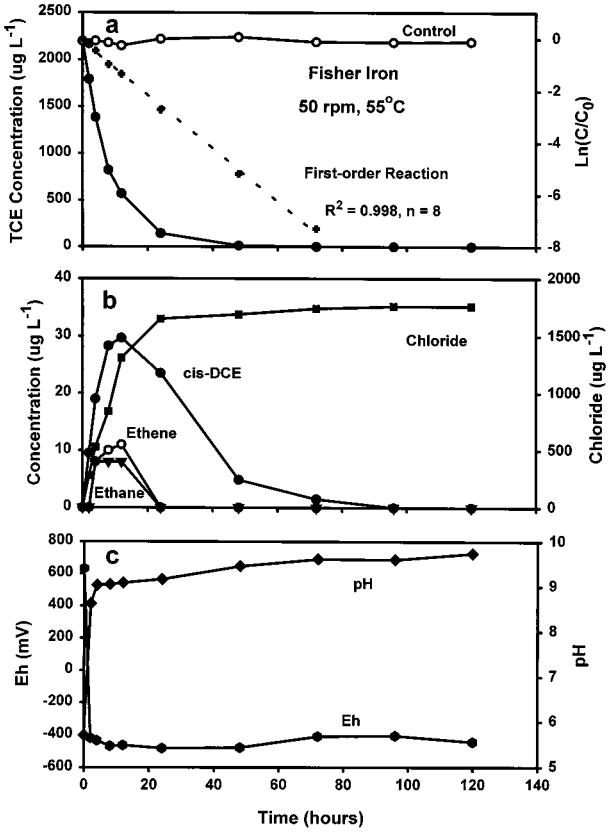

FIGURE 3. Kinetics of TCE reduction by pristine Fisher Fe^0 at 50 rpm and 55 °C: (a) TCE concentration and the pseudo-first-order equation fit of the data, (b) reaction byproducts, and (c) pH and Eh.

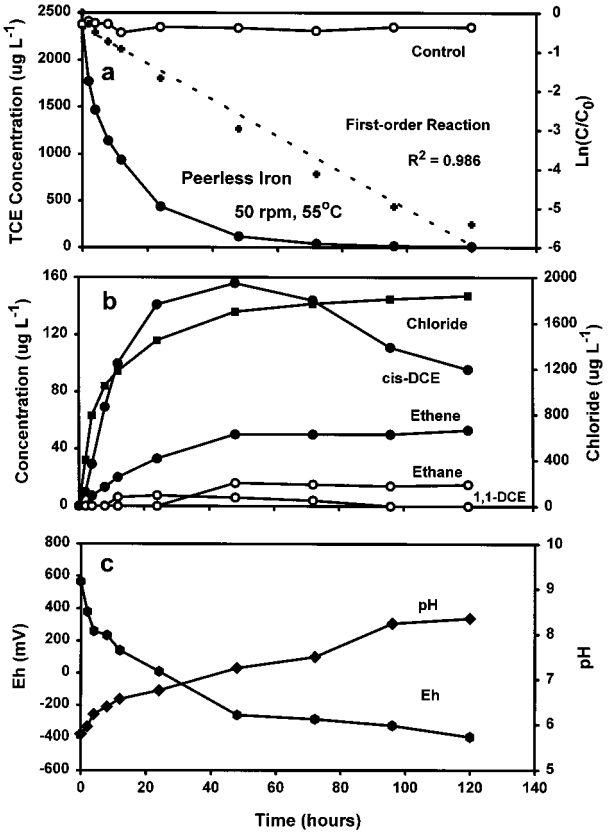

FIGURE 4. Kinetics of TCE reduction by pristine Peerless Fe^0 at 50 rpm and 55 °C: (a) TCE concentration and the pseudo-first-order equation fit of the data, (b) reaction byproducts, and (c) pH and Eh.

increased with a corresponding decrease in TCE over time. Concentrations of Fe^{3+} and Fe^{2+} were below the detection limits. Trends in pH and Eh are shown in Figure 2c. The pH increased rapidly from an initial value of 5.7 to 9.1 after 12 h and then leveled off. Conversely, Eh decreased from an initial value of 660 to −320 mV within the first 4 h and remained constant at about −400 mV afterward. Results for TCE degradation by Fisher Fe^0 at 55 °C are shown in Figure 3. The TCE showed a faster decline at 55 °C than at 25 °C, and no TCE was detected after 96 h at 55 °C (Figure 3a). The concentrations of *cis*-DCE, ethene, and ethane showed maxima from 8 to 12 h (Figure 3b). The maxima in ethane and ethene values were most likely the result of loss through a headspace generated in 8 h by hydrogen gas produced by iron decomposition of water. Slightly higher pH and lower Eh values were observed at 55 °C than at 25 °C (Figure 3c).

The test results for Peerless Fe^0 at 55 °C are presented in Figure 4. Similar results were obtained for the Master Builders Fe^0. Slower TCE reduction kinetics was evident for the Peerless Fe^0 relative to the Fisher Fe^0 at the same temperature despite the fact that the former had a surface area of 7.7 times of the latter. Both *cis*-DCE and 1,1-DCE were present as reaction products (Figure 3b). The pH gradually increased from an initial value of 5.7 to 8.4 at 120 h, whereas the Eh gradually decreased to −400 mV at the end of run. The gradual changes in both pH and Eh for the Peerless Fe^0 contrast with abrupt changes for the Fisher Fe^0. The difference could be due to the degree of surface (hydr)oxide layer and the amount of reactive surface sites other than the total surface area of the metal involved in the TCE reduction. Metal oxide (e.g., magnetite), hydroxide, and oxyhydroxide that form on the surface of the metal tend to passivate the Fe^0 surface and protect it from further oxidation by water and contaminant. Visual inspection and SEM examination revealed that the Peerless Fe^0 was air-oxidized to a greater degree than the Fisher Fe^0.

Figure 5 gives the data on the TCE reduction by Fisher Powdered Sn^0 at 55 °C. The reaction products included *cis*-DCE, *trans*-DCE, VC, and ethene (Figure 5b). The pH of the solution went down from an initial value of 5.7 to 5.1 in 2 h and then went up gradually to 5.9 in 120 h (Figure 5c). The Eh dropped from 680 mV in the beginning to 170 mV in 120 h. No negative Eh values were found in any of the Sn^0 systems at all four temperatures.

In all cases, from 90 to 110% of the chlorine atoms present in the starting TCE solution in both Fe^0 and Sn^0 systems were accounted for by free chloride ions and DCE isomers. Detected intermediate and final products are listed in Table 3. *cis*-DCE was the only detected chlorinated byproduct of TCE transformation by Fisher and Master Builders Fe^0, whereas 1,1-DCE was also found in the Peerless Fe^0 system. *trans*-DCE and VC were also detected in the Fisher powdered Sn^0 system at 55 °C. Traces of acetylene were found in some runs (Table 3). The absence of ethene and ethane in some treatments at 25 °C (Table 3) could be a result of low sensitivity of our method for dissolved gas analysis.

Campbell et al. (*15*) proposed the following pathways for TCE reductive dechlorination by Fe^0: (a) reductive β-elimination reaction $\{R(X)\text{═}R(X) + 2e^- \rightarrow R \equiv R + 2X^-\}$; (b) hydrogenolysis reaction $\{R(X) + 2e^- + H^+ \rightarrow RH + X^-\}$; (c) reduction of triple bond to olefin $\{R \equiv R + 2e^- + 2H^+ \rightarrow RH\text{═}RH\}$; and (d) reduction of triple bond to alkane $\{R \equiv R + 4e^- + 4H^+ \rightarrow R(H_2)\text{-}R(H_2)\}$. Our results seem to support their scheme, and the same pathways should also be operative in the Sn^0 system. There were generally more *cis*-DCE and *trans*-DCE as TCE's daughter products in the Sn^0 treatment relative to the Fe^0 treatment, suggesting a greater portion of

TABLE 3. Intermediate and Final Degradation Products of TCE by Untreated and HCl-Washed Fe^0 and Sn^0

material	temperature	
	25 °C	55 °C
Fisher Fe^0	cis-DCE, ethene, ethane, chloride	cis-DCE, ethene, ethane, chloride
Masters Builders Fe^0	cis-DCE, ethene, chloride	cis-DCE, ethene, ethane, chloride
Peerless Fe^0	cis, 1,1-DCE, ethene, ethane, chloride	cis 1,1-DCE, ethene, ethane, chloride
Aldrich Fe^0	chloride	1,1-DCE, ethene, chloride
Fisher powdered Sn^0	chloride	cis,trans-DCE, VC, acetylene, ethene, chloride
Aldrich powdered Sn^0	cis,trans-DCE, chloride	cis,trans-DCE, ethene, chloride
Aldrich granular Sn^0	chloride	cis,trans-DCE, VC, ethene, chloride
Fisher Fe^0 + Sn^0 (1:1)	cis-DCE, acetylene, ethene, ethane, chloride	cis,trans-DCE, ethene, ethane, chloride
Fisher Fe^0 (HCl)	cis-DCE, ethene, ethane, chloride	cis-DCE, ethene, ethane, chloride
Master Builders Fe^0 (HCl)	ethene, ethane, chloride	cis-DCE, ethene, ethane, chloride
Peerless Fe^0 (HCl)	cis-DCE, ethene, ethane, chloride	cis-DCE, ethene, ethane, chloride
Aldrich Fe^0 (HCl)	chloride	ethene, ethane, chloride
Aldrich granular Sn^0 (HCl)	chloride	cis,trans-DCE, chloride

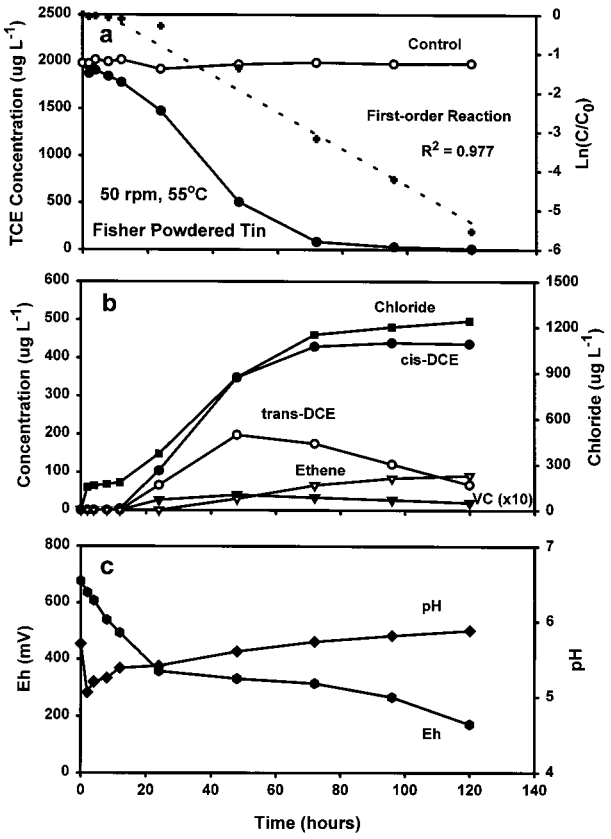

FIGURE 5. Kinetics of TCE reduction by pristine Fisher powdered Sn^0 at 50 rpm and 55 °C: (a) TCE concentration and the pseudo-first-order equation fit of the data, (b) reaction byproducts, and (c) pH and Eh.

TCE going through β-elimination reaction by Fe^0 than by Sn^0.

Acknowledgments

Although the research described in this article has been funded wholly or in part by the USEPA, it has not been subjected to the Agency's peer and administrative review and therefore may not necessarily reflect the views of the Agency and no official endorsement may be inferred. The senior author acknowledges the National Research Council Resident Research Associateship program. We wish to acknowledge gratefully the analytical assistance and support of the following staff of ManTech Environmental Research Services Co.: Randy Callaway, Steve Vandegrift, Linda Pennington, Lisa Hopkins, Ming Ye, Priscilla Rodebush, and Mark White.

Literature Cited

(1) Gillham, R. W.; O'Hannesin, S. F. *Ground Water* **1994,** *32,* 958−967.
(2) Puls, R. W.; Powell, R. M. 1997. Permeable Reactive Subsurface Barriers for the Interception and Remediation of Chlorinated Hydrocarbon and Chromium (VI) Plumes in Ground Water. EPA Remedial Technology Fact Sheet. Ada, OK. EPA/600/F-97/008.
(3) O'Hannesin, S. F.; Gillham, R. W. *Ground Water* **1997,** *36,* 164−170.
(4) Boronina, T.; Klabunde, K. J. *Environ. Sci. Technol.* **1995**, *29,* 1511−1517.
(5) Johnson, T. J.; Scherer, M. M.; Tratnyek, P. G. *Environ. Sci. Technol.* **1996,** *30,* 2634−2640.
(6) Tratnyek, P. G.; Johnson, T. L.; Scherer, M. M.; Eykholt, G. R. *Ground Water Monit. Remed.* **1997,** *17*(4), 108−114.
(7) Lasaga, A. C. *J. Geophys. Res.* **1984,** *89,* 4009−4025.
(8) Laidler, K. J. *Chemical Kinetics*; McGraw-Hill: New York, 1965; p 205.
(9) Sivavec, T. M.; Horney, D. P. *Natl. Meet.-Am. Chem. Soc., Div. Environ. Chem.* **1995,** *35(1),* 695−698.
(10) Scherer, M. M.; Westall, J. C.; Ziomek-Moroz, M.; Tratnyek, P. G. *Environ. Sci. Technol.* **1997,** *31,* 2385−2391.
(11) Orth, W. S.; Gillham, R. W. *Environ. Sci. Technol.* **1996,** *30,* 66−71.
(12) Matheson, L. J.; Tratnyek, P. G. *Environ. Sci. Technol.* **1994,** *28,* 2045−2053.
(13) Schreier, C. G.; Reinhard, M. *Chemosphere* **1994,** *29,* 1743−1753.
(14) Roberts, A. L.; Totten, L. A.; Arnold, W. A.; Burris, D. R.; Campbell, T. J. *Environ. Sci. Technol.* **1996,** *30,* 2654−2659.
(15) Campbell, T. J.; Burris, D. R.; Roberts, A. L.; Wells, J. R. *Enriron. Toxicol. Chem.* **1997,** *16,* 625−630.
(16) Ye, M. Y.; Shen, Y.; West, C. C.; Lyon, W. G. *J. Liq. Chrom. Relat. Technol.* **1998,** *21*(4), 551−565.
(17) Agrawal, A.; Tratnyek, P. G. *Environ. Sci. Technol.* **1996,** *30,* 153−160.
(18) Burris, D. R.; Campbell, T. J.; Manoranjan, V. S. *Environ. Sci. Technol.* **1995,** *29,* 2850- 2855.
(19) Johnson, T. L.; Fish, W.; Gorby, Y. A.; Tratnyek, P. G. *J. Contamin. Hydro.* **1998,** *29,* 379−398.
(20) Spiro, M. In *Chemical Kinetics, Vol. 28, Reactions at the Liquid−Solid Interface;* Compton, R. G., Ed.; Elsevier: Amsterdam, 1989; pp 69−166.
(21) Pilling, M. J.; Seakins, P. W. *Reaction Kinetics*; Oxford University Press: New York, 1995; p 151.
(22) Sparks, D. L. *Kinetics of Soil Chemical Processes*; Academic Press: San Diego, 1989; p 31.
(23) Liang, L.; Korte, N.; Goodlaxson, J. D.; Clausen, J.; Fernando, Q.; Muftikian. *Groundwater Monit. Remed.* **1997,** *17*(1), 122−127.

Received for review May 12, 1998. Revised manuscript received October 12, 1998. Accepted October 19, 1998.

ES980481A